Modeling of Coal Liquefaction Kinetics Based on Reactions in Continuous Mixtures

Part II: Comparison with Experiments on Catalyzed and Uncatalyzed Liquefaction of Coals of Different Rank

Experimental kinetic data for three Australian coals are compared with predictions from the mathematical model developed in Part I. For these coals, as well as data reported for North American coals, the model is found to show good agreement, using the characteristic molecular weight as the only parameter. The effects of reaction time and temperature are coupled via a severity index that arises in the model as a dimensionless reaction time. The model is also shown to be applicable when catalysts are present. The product distribution for a particular coal seems to be a function only of the conversion even in the presence of catalysts, as long as the chemical reaction controls the rate of liquefaction.

G. N. Prasad, J. B. Agnew, T. Sridhar
Department of Chemical Engineering
Monash University, Wellington Road
Clayton 3168, Australia

SCOPE

Conventional coal liquefaction kinetic modeling is based on the grouping together of products into several "lumps," usually determined by the solubility properties of the various species present. The reaction networks for such a lumped-product system depend clearly on the particular coal and it is not possible to generalize such models. In Part I, a model based on the concept of reactions in a continuous mixture was proposed and a methodology of applying such a model was developed.

In this paper, the product distributions obtained upon liquefaction of three Australian coals—a low-rank Victorian brown coal and two subbituminous coals—are examined and compared with model predictions using the model developed in Part I and the lumping functions proposed therein. The kinetic data were obtained from two different types of reactors, a tubular flow reactor and a batch microautoclave reactor. All experiments were conducted under conditions where there was excess availability of hydrogen from donor solvent (tetralin). In addition, other reported kinetic data for North American coals were examined. The effect of catalyst addition (mostly iron-based), is also examined and the applicability of the model is evaluated.

CONCLUSIONS AND SIGNIFICANCE

The model proposed in Part I is found adequate in predicting the product distribution for all coals examined. The only parameter varied between different coals is the characteristic molecular weight for coal. The molecular weight for coal broadly depends upon the rank, and increases as the rank increases.

The model provides a basis for coupling the effects of reaction time and temperature using the concept of severity index. The implication for liquefaction of coal is that there is no optimum temperature for maximizing the yield of a particular product as long as the solvent is capable of supplying all the hydrogen requirements.

Correspondence concerning this paper should be addressed to T. Sridhar.
J. B. Agnew is presently at the Department of Chemical Engineering, University of Adelaide, Adelaide, 5001, Australia.

The product distribution is uniquely determined by reaction severity. This implies that the activation energy is similar for all reactions in the network.

The first-order rate constant for the formation of tetrahydrofuran (THF) solubles (defined as the liquefaction products) for different coals is found to follow an Arrhenius relationship. The activation energy for this rate parameter is a unique function of coal being primarily dependent upon the atomic hydrogen/carbon (H/C) ratio of coal.

The effect of added catalysts in the presence of a good donor solvent is shown to accelerate all reactions equally, without altering the selectivity. The predicted profiles for both catalyzed and uncatalyzed reactions are found to be the same at the same conversion level. The beneficial effect of catalyst may however be more pronounced when solvents of poor quality such as recycle solvents are used. It follows that the catalyst function in such applications is primarily to promote hydrogen transfer reactions in the solvent.

Background

There have been numerous attempts to identify factors that would correlate coal properties with their behavior during liquefaction. Neavel's work (1976) on liquefaction of a suite of coals indicated a relationship between coal rank and conversion. Given and coworkers (1980) studied a wide suite of coals in an attempt to establish parameters capable of correlating liquefaction behavior of different coals. Furlong et al. (1982) have proposed a kinetic method of correlating reactivities of different coals based on a fitted second-order rate constant for a reversible scheme. Despite extensive efforts, no universal index of coal reactivity has been found.

In Part I a generalized coal liquefaction model was developed where, in the presence of an excess available hydrogen supply (as in a good donor solvent), one would essentially study the thermal reactions of coal. In the model formulation we defined a parameter α characteristic of the rate of breakdown of the original coal. For coals made up of similar structural units α would be a good indicator of the reactivity. Coals of a particular rank would have similar basic unit structures within the matrix and hence be likely to yield products of similar nature.

In coal liquefaction, the role of catalyst is attributed variously as promoting the rehydrogenation of donor solvent using gas-phase hydrogen (Guin et al., 1978; Rottendorf and Wilson, 1980) or capping of reactive fragments produced from thermal cracking of coal using gas-phase hydrogen (Cassidy et al., 1982; Cochran et al., 1982; Moritomi et al., 1983) or promotion of coal-tetralin reactions (Tsai and Weller, 1979). Recently Brooks et al. (1983), while examining the effect of pyrite catalysts using a Pittsburg No. 8 coal and model compounds, found these catalysts to accelerate all three reactions mentioned above, especially those involving molecular hydrogen from the gas phase.

The conventional approach in modeling the kinetics of reaction in all cases would involve writing a network for the lumped products and estimating the optimum set of parameters that best correlate the data. Such a procedure, due to its empirical nature, would not allow any generalization based on the lumped models. With this background, a model based on the concept of reactions in continuous mixtures (Aris and Gavalas, 1966) was developed in part I to simulate the reactions occurring during liquefaction of coal.

In the following sections we evaluate the predictions of the model developed in Part I with the experimental results obtained from liquefaction of three Australian coals, a Victorian brown coal from the Morwell seam and two subbituminous coals from Queensland. The effect of catalysts on the kinetics of product formation for the brown coal is also examined. Literature data on the liquefaction of coals of different rank carried out in the presence of an excess amount of tetralin as the donor solvent are also used in the model evaluation, both in the presence and absence of catalysts.

Experimental

The kinetic data for brown coal were obtained from two types of reactors. A continuous-flow tubular bubble-column reactor with external jackets for heating was employed to provide well-defined reaction time and temperature. The detailed description of the bubble column, operational experience, and the results from some of the runs have been presented elsewhere (Agnew et al., 1984). The flow characteristics and the hydrodynamic behavior of the bubble column under coal-liquefaction conditions have been well examined (Sangnimnuan et al., 1984). Two tubular vessels of 19 and 12 mm ID were employed to obtain a range of residence times in the reactor. Since there was some axial temperature variation, an equivalent isothermal temperature was calculated. In the range of operating conditions employed, the reactor can be considered essentially as plug-flow in nature, with Peclet numbers greater than 5 for the 19 mm column and greater than 10 for the 12 mm column.

A batch microreactor, 19 mm ID and 125 mm long, was employed to obtain short reaction-time data for the brown coal, and complete kinetic data for the two Australian subbituminous coals. To provide rapid heatup rates, a fluidized sand bath was used as the heating medium. Thorough mixing within the reactor was ensured by using a pneumatically actuated shaker.

Materials

Samples of a Victorian brown coal from the Morwell seam (supplied by the Victorian Brown Coal Council) were used in the experiments. Drum 289 of the 1979 100 metric ton bulk sample was used. The analysis of this coal and the two high-volatile subbituminous coals, Wandoan and Taroom, used in this study are summarized in Table 1. All coals were specifically chosen for their low sulfur contents and were oven-dried (at 110°C) and ground to <74 μm before use.

The kinetic data for all the coals were obtained using a 3:1 ratio of tetralin to coal under a hydrogen atmosphere. Details of the slurry preparation and the continuous reactor operation (at 10 MPa) are presented elsewhere (Agnew et al., 1984). For the runs carried out with the microreactor, 6 g of tetralin and 2 g of

Table 1. Analysis of Morwell, Wandoan, and Taroom Coals

	Coal		
	Morwell	Wandoan Source	Taroom
Element	Morwell Victoria	Austinvale Sturt Basin Queensland	Northern Sturt Basin Queensland
	Ultimate Analysis (wt. % DAF basis)		
Carbon	70.4	77.4	76.15
Hydrogen	4.9	5.99	5.94
Sulfur	0.3	0.48	0.43
Nitrogen	0.5	1.08	1.17
Oxygen (diff.)	23.9	15.1	16.4
Ash	3.4	9.4	7.4

coal were used and the reactor was initially pressurized to 4 MPa with hydrogen. To establish that sufficient hydrogen donor solvent was present in the microreactor, a higher tetralin charge was used and found to yield no improvements in conversion.

The kinetic data for the catalyzed liquefaction were obtained from the tubular flow reactor using cheap iron-based catalysts added via ion-exchange methods reported earlier (Agnew et al., 1984).

Product analysis and data base

The liquid and solid products were analyzed using the solvent extraction method (Jackson et al., 1983), which is summarized in Figure 1. The gaseous products were analyzed for carbon oxides as well as hydrocarbons using a Varian gas chromatograph equipped with a flame ionization detector and a thermal conductivity detector.

The data base for the brown coal included results from the work carried out at Monash University by various investigators over the past five years (Agnew et al., 1984; White et al., 1982; Thewlis et al., 1983). Results obtained at identical conditions of temperature and time using the flow reactor and microreactor were found to agree very well. This observation lends further support of negligible backmixing in the flow reactor and hence the assumption of plug flow of the reactor contents. Further it suggests that gas phase hydrogen may not be a limiting reactant

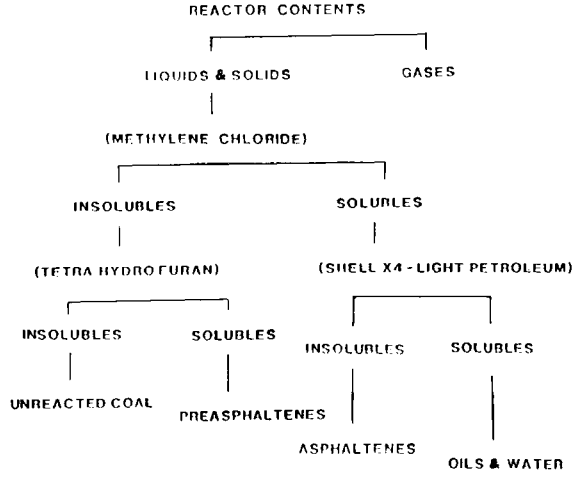

Figure 1. Product analysis and classification.

contributing to hydroliquefaction reactions under these conditions. As reported by Gollakota and Guin (1984), in coal liquefaction reactors the mass transfer coefficient can vary signficantly due to the type of contactor used, and the compatibility between the microreactor results and bubble-column reactor results confirms that the hydrogen donor solvent, tetralin, is effective in providing all the hydrogen necessary to stabilize the reactive fragments produced during coal liquefaction. Thus one is studying, in effect, the thermal reactions of coal.

Table 2 contains a summary of elemental analyses of the coals used by other investigators who have published kinetic data for coal liquefaction in batch or plug-flow reactors. All these investigators have employed tetralin as a model donor solvent and no external catalyst was used. The product distribution was mostly reported in terms of solubility-based criteria. However, Mohan and Silla (1981) and Leonard and Silla (1983) presented the product yields in terms of functional groups obtained by chromatography.

Reproducibility

Since there was a large data base available for brown coal, a reproducibility check was made to estimate the expected error bounds associated with the experimental data. All repeated results were examined. The deviation for each sample i at a particular temperature and reaction time was calculated. An overall average deviation for all the product fractions was calculated for n_i number of repeated runs for sample i: Average deviation = $[n_i \text{ X (deviation in sample)}]_i/\Sigma n_i$.

It was generally found that as the numerical value of product fraction increased the error bounds decreased. The average deviation calculated using the above procedure yielded error bounds for conversion (±4%), preasphaltenes (±8.8%), and asphaltenes (±9.0%).

Since the oils, gases, and water (OGW) fraction was obtained by difference, the uncertainty for this fraction was estimated using the maximum probable error (MPE) method outlined by Holman and Gajda (1978). The estimated uncertainty for OGW fraction was ±10.5%.

Results and Discussion

Rate of coal dissolution

Brown Coals. According to the model formulation, all tetrahydrofuran (THF) insolubles are assumed to be unreacted coal. The experimental data over the range 588 to 688 K are presented in Figure 2 along with the predicted values based on first-order kinetics. It has to be noted that these predictions are based on zero initial concentration of THF solubles and complete conversion of THF insolubles at infinite time. It can be seen that such predictions do not adequately represent the experimental data.

Figure 3 contains the data corrected for the initial rapid conversion, assuming a 10% initial THF soluble product, along with first-order fitted values based on 10% THF solubles at zero reaction time. The fit is clearly better at short reaction times. This 10% instantaneous dissolution for brown coal can be attributed to physical extraction along with scission of very weak linkages present in the coal matrix. In low-rank coals such an assumption seems consistent with the idea of a more extensive network of relatively weak bonds as compared with higher ranking coals. Zieminski (1982) has offered a similar explanation for the ini-

Table 2. Summary of Reported Liquefaction Kinetic Studies*

	Coal				
	Madisonville #9 Kentucky	Utah	Pittsburgh Seam W. Virginia Investigators	Kentucky #6	Illinois #6
Element	Shalabi et al. (1979)	Wiser & Hill (1967)	Curran et al. (1967)	Leonard & Silla (1983)	Mohan & Silla (1981)
	Ultimate Analysis (wt. % Moisture-Free Basis)				
Carbon	55.89	72.88	71.77	75.2	68.9
Hydrogen	4.30	5.58	4.86	5.2	4.8
Sulfur	4.92	0.65	2.48	2.6	3.7
Nitrogen	0.87	1.51	1.25	1.7	1.2
Oxygen	8.79	10.82	7.12	8.2	8.9
Ash	25.23	8.37	12.52	7.1	12.5

*Uncatalyzed batch/PFR using tetralin.

tial rapid step of extracting ca. 10–15% of DAF (dry ash free basis) coal that involved a low activation energy (ca. 42 kJ/mol). Szladow and Given (1983) have adopted a similar procedure for correcting the zero-time yields of pyridine solubles.

The usual approach to modeling coal conversion data is to assume a temperature-dependent maximum conversion (Shalabi et al., 1979; Cronauer et al., 1978; Han et al., 1978). Thus a pseudoreversibility concept is incorporated in these models. Although such an approach would allow an additional parameter whereby a good first-order fit would be obtained for THF conversion plots, we feel that such an explanation is not totally justified. However, following Szladow and Given (1981, 1983), we use a temperature-independent maximum attainable conversion that corresponds to the reactive portion of coal. Looking at the data for the highest temperature and longest time, Figure 3, we find that essentially all of the THF insolubles are consumed. Hence there appears to be no "refractory-unreactive portion" in brown coal.

The first-order rate constant for the formation of THF solubles at each of the temperatures was estimated using an IMSL (1982) routine based on a finite-difference Levenberg-Marquadt algorithm. Figure 3 shows the fit between the experimental data and the predicted conversion.

Australian Subbituminous Coals. Figures 4 and 5 contain conversion-time plots for Wandoan and Taroom coals, respectively. Unlike the brown coal, the conversion at the highest temperature and longest reaction time asymptotes to a value less than 100%. Based on this asymptotic value we estimate the temperature-independent reactive fraction (DAF basis) for these coals as 91% for Wandoan and 93% for Taroom coal. These values are slightly higher than those for bituminous coals, between 85–90% as reported by Han and Wen (1979) and 89% as reported by Szladow and Given (1981).

Model parameters

In the model developed in Part I, the following functions were used for the rate and stoichiometric kernels:

$$K(x_1, x_2) = [(x_1 + x_2)^2/(u + v)^2] \cdot \alpha \qquad (1a)$$

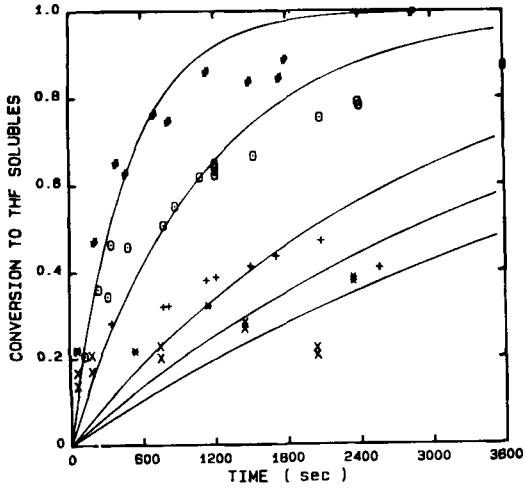

Figure 2. Morwell coal conversion (MAF basis) vs. reaction time.
Comparison with first-order model (zero initial THF solubles).
×, 315°C; *, 335°C; +, 375°C; ⊙, 395°C; #, 415 C

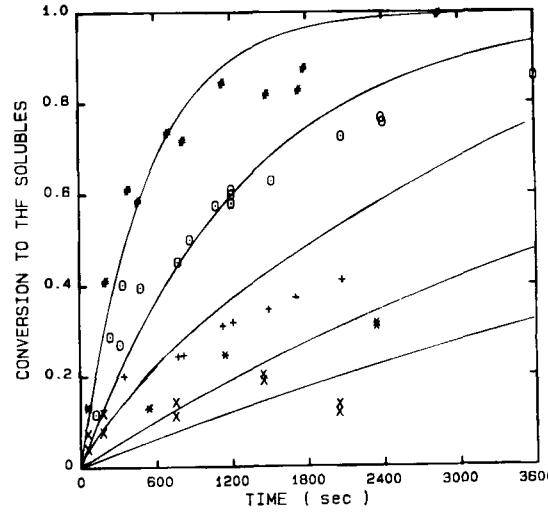

Figure 3. Morwell coal conversion (MAF basis) vs. reaction time.
Comparison with first-order model (10% initial THF solubles).
×, 315°C; *, 335°C; +, 375°C; ⊙, 395°C; #, 415 C

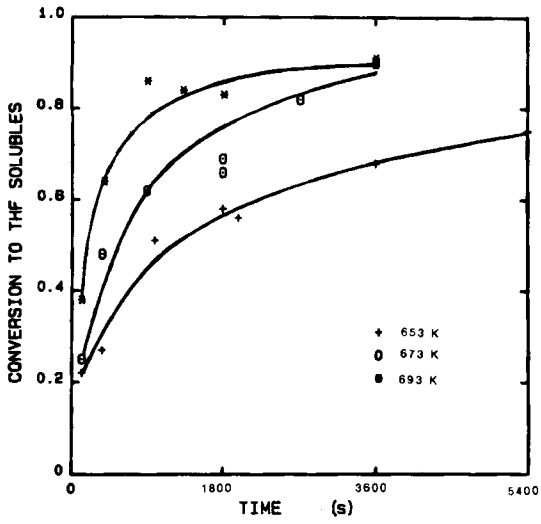

Figure 4. Wandoan coal conversion (MAF basis) vs. reaction time.

and

$$\nu(x_1', x_2'; x_1, x_2) = \frac{12}{(x_1^3 x_2 + x_1 x_2^3)} [x_1'(x_1 - x_1') + x_2'(x_2 - x_2')] \quad (1b)$$

The solubility functions that were used to obtain lumped products were,

$$L_1 = \gamma_1 \cdot (12x_1 + 16x_2)^{-1} \quad (2a)$$

$$L_2 = \gamma_2 \cdot (12x_1 + 16x_2)^{-1} \quad (2b)$$

There are three parameters that can be varied independently to fit the three lumped-product distributions. One of these is a characteristic molecular weight for coal, which is required to obtain the continuous reaction model's prediction of product distribution as a function of carbon and oxygen atoms per molecule. The other two parameters are γ_1 and γ_2 in Eq. 2 that arise in lumping the continuous product distribution to the lumped products, preasphaltenes, asphaltenes, and OGW fraction. As discussed in Part I, these two parameters (γ_1 and γ_2) arise due to the classification based on solubility; they are solvent-dependent and hence should be kept independent of coal.

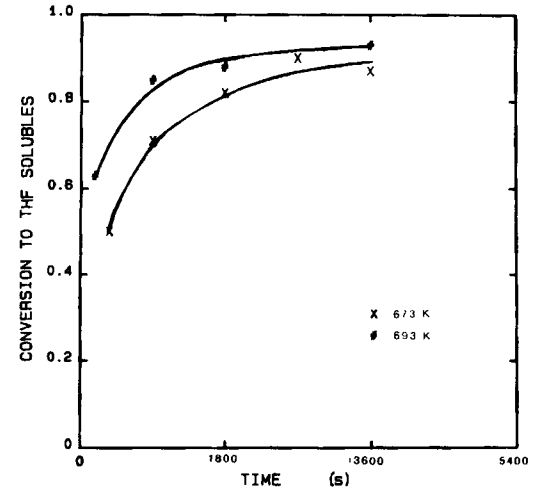

Figure 5. Taroom coal conversion (MAF basis) vs. reaction time.

Recently Lucht and Peppas (1984) have proposed a crosslinked macromolecular network model for coal. They proposed that a coal macromolecule was comprised of hypothetical repeating units somewhat analogous to a polymer. The number-average molecular weight between crosslinks, $\overline{M}_c$, for coal was obtained using a modified Gaussian network equation (Lucht and Peppas, 1981). Using the equilibrium swelling of pyridine-extracted coal samples Lucht and Peppas (1984) calculated $\overline{M}_c$ for coals of varying carbon content. The results show a correlation between $\overline{M}_c$ and percent carbon content over a range of 70 to 82.5% carbon [DMMF (dry mineral matter free) basis]. Since the molecular weight between crosslinks is somewhat analogous to the characteristic molecular weight of coal that we have proposed in the present model, we choose a value close to 1,000 (at 70% C content) as the molecular weight of brown coal.

The actual molecular weight used in the model simulation for brown coal was 1,036 (with calculated carbon and oxygen contents based on the elemental composition of $u = 65$ atoms and $v = 16$ atoms, respectively). The parameters ($\gamma_1 = 200$ and $\gamma_2 = 400$) were found to yield model-predicted lumped components matching the experimental values. Once these parameter values were determined for the brown coal, they were used for all other coals studied here. The characteristic molecular weight of coal was the only parameter that was varied to simulate the product distribution for other coals.

It should be noted that the combination of parameters fitted for brown coal is not unique since, as observed in Part I, use of a higher value for the characteristic molecular weight along with appropriate values for γ_1 and γ_2 would have led to similar fits. Hence one should exercise care in interpreting the absolute values of the molecular weights of the products predicted by the model, which would all be under 1,000, being less than the coal itself. However, the relative molecular weights of the various lumped fractions and the relative change within a lumped fraction as a function of reaction time and temperature should be compared with the experimental results.

Reaction severity and product yields

Brown Coals. In the development of the continuous reaction model we arrived at the dimensionless form of the model equation leading naturally to a dimensionless time θ. This definition of dimensionless time couples the effects of reaction temperature (via α) and reaction time t and can be considered as a reaction severity index (SI):

$$\text{SI} = \theta = \alpha \cdot t$$

$$\text{SI} = \begin{matrix}\text{rate constant for} \\ \text{formation of THF} \\ \text{solubles } (\alpha)\end{matrix} \times \begin{matrix}\text{reaction} \\ \text{time, } t\end{matrix} \quad (3)$$

With such a definition it is possible to construct a generalized plot of conversion to THF soluble products (defined as unreacted coal). Figure 6 shows such a plot using all the experimental data from the continuous-flow reactor and the batch

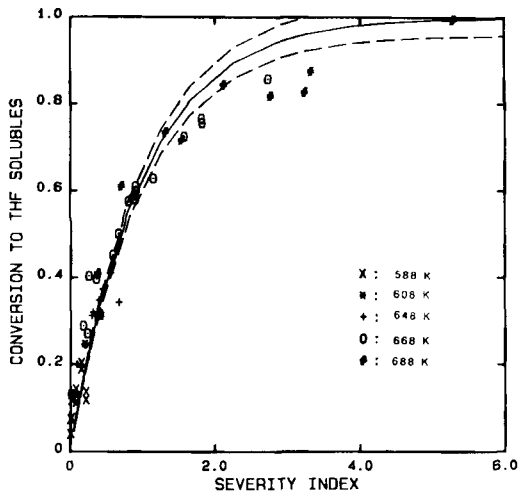

Figure 6. Model fit for conversion of Morwell coal.

microreactor. The solid line indicates the first-order coal consumption model fit and the broken lines indicate the ±4% deviation estimated from the experimental data on reproducibility. Large deviation between the experimental points and the theoretical line is a direct consequence of the poor fit of Figure 3.

Based on our definition of reaction severity index, generalized plots for the lumped products can be constructed. Figure 7 contains the experimental data for the fractional yields of preasphaltenes, asphaltenes, and the OGW fraction obtained from liquefaction of brown coal. Included on this plot are the predicted curves obtained by using the parameters stated earlier. The bounds of uncertainty on the experimental data are shown by broken lines on either side of the solid line. Bearing in mind the diversity of the data base that includes two different reactor

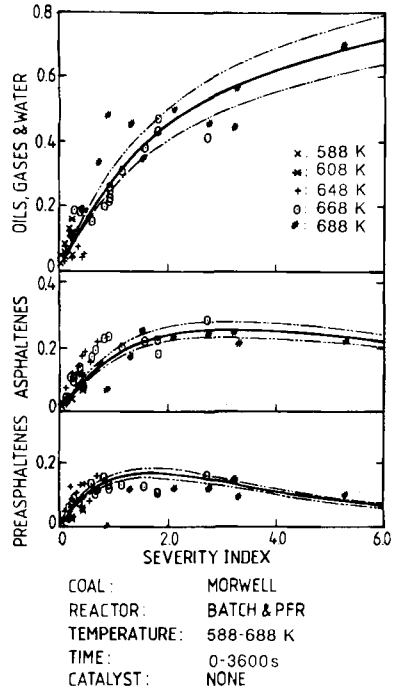

Figure 7. Model fit for product yields (Morwell coal).
Broken lines are estimated uncertainties in data.

systems from three different investigators over a wide range of temperatures (588 to 688 K) and reaction times (0 to 3,600 s), the fit between the model and experiment is quite good.

The model predicts the simultaneous formation of a spectrum of products (as observed for a Texas lignite by Phillip and Anthony, 1982) without recourse to formation of intermediate pseudocompounds such as preasphaltenes, asphaltenes, etc. This has been achieved without introducing too many parameters, using a conceptually advanced model. The concept of reaction severity index arises naturally in the model. A coupling effect of reaction temperature and time as arising in the severity index has been recognized by Petrakis et al. (1983). Figure 8 shows a plot of preasphaltenes fraction against the severity index due to Petrakis et al.:

$$\text{SI} = 2 \times \text{reaction time (min)} + \text{temperature (°C} - 400) \quad (4)$$

Comparing Figure 8 with the corresponding Figure 7 one can readily see that the severity index arising from our model is at least as effective in coupling the effects of reaction temperature and time as that of Petrakis et al. Admittedly, as pointed out by Petrakis et al., their severity index was empirically derived to correlate their data without any theoretical justification for their choice, and as such cannot be expected to be universally valid.

Australian Subbituminous Coals. Based on the definition of severity index, a generalized plot for the conversion to THF solubles can be constructed. Such a plot is shown in Figure 9, which includes the data from both Wandoan and Taroom coals. Included in the plot is the theoretical curve predicted by the first-order irrversible model. We note that in this plot the data have been expressed as a fraction of the reactive portion in coal estimated earlier.

Figure 10 contains plots of weight fractions of preasphaltenes, asphaltenes, and OGW fraction obtained for the Wandoan coal; the corresponding data for the Taroom coal are shown in Figure 11. As in the case of brown coal, the severity index seems to reasonably couple the combined effects of reaction temperature and time for the two coals over the range studied. The predicted profiles for all product fractions are shown as solid line in these figures. These theoretical profiles were obtained by choosing an appropriate value for the characteristic molecular weight of coal in each case to fit the experimental preasphaltenes fraction. Once a good fit was obtained for the preasphaltenes, the rest of the lumped product profiles were predicted. Thus molecular weight was the only parameter that was varied between the different coals.

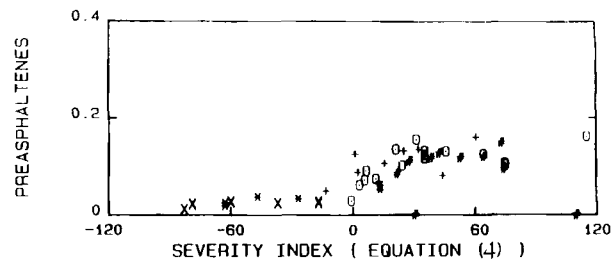

Figure 8. Preasphaltenes yield for Morwell coal vs. Eq. 4.
Symbols as in Fig. 2.

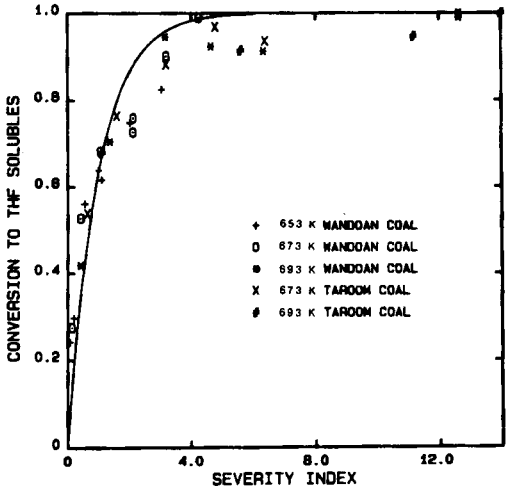

Figure 9. Model fit for conversion.
Wandoan and Taroom coals.

The fit between the experimental and predicted product yields is quite remarkable, especially when one considers that only a single parameter (the characteristic molecular weight) has been changed for different coals. Table 3 contains a summary of the parameters used for different coals. It should be noted that the carbon and oxygen contents were assigned for each coal based on the assumed molecular weight and using the elemental analysis. The use of a higher molecular weight for the subbituminous coals as compared with the brown coal can be reconciled in terms of an increase in the degree of condensed structure with increase in carbon content leading to a larger molecular mass per macromolecule of coal (Lucht and Peppas, 1984).

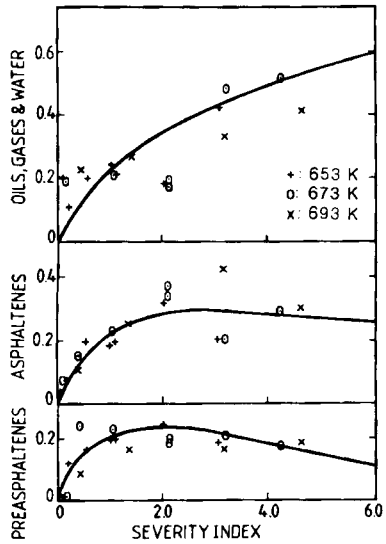

Figure 10. Model fit for product yields.
Wandoan coal.

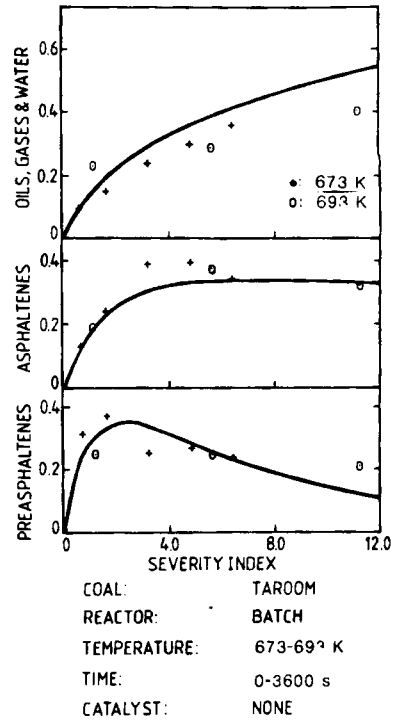

Figure 11. Model fit for product yields.
Taroom coal.

North American Coals. Of the investigators listed in Table 2, only Shalabi et al. (1979) used a three-solvent method of fractionating reaction products similar to the present work. While conversion of coal was defined in terms of THF solubles, these investigators used benzene and pentane to obtain the lumped product fractions. Figure 12 shows their data plotted as a fraction of the DAF "reactive coal" basis. The reactive fraction being estimated as 88% of DAF coal obtained at the most severe reaction condition. As in the case of the other coals, the severity index is found to be effective in coupling the temperature and the time effects.

The model-predicted profiles are shown in Figure 12 as solid lines and were obtained using a higher characteristic molecular weight for the Kentucky No. 9 coal studied by Shalabi et al. (1979). As before, all other parameters were kept constant (Ta-

Table 3. Summary of Model Parameters Used for Different Coals

Coal	γ_1	γ_2	Molecular Weight	u (No. Carbon Atoms)	v (No. Oxygen Atoms)
Morwell brown coal	200	400	1,036	65	16
Wandoan coal	200	400	1,212	85	12
Taroom coal	200	400	1,820	125	20
Kentucky #9 (Shalabi et al., 1979)	200	400	2,088	150	18
Pittsburg coal (Brooks et al., 1983)	200	400	1,328	100	6

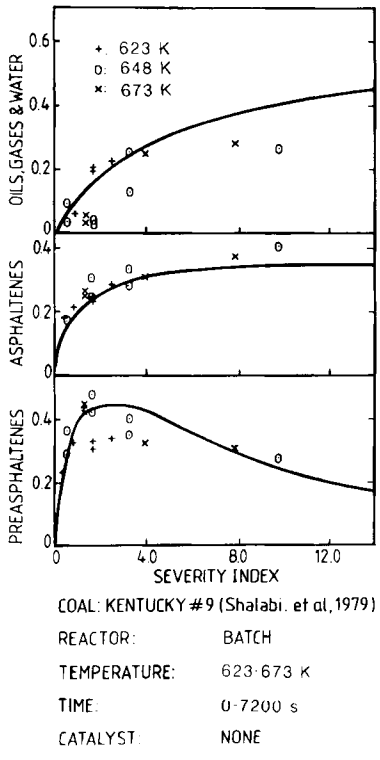

Figure 12. Model fit for poduct yields.
Kentucky No. 9 Coal; Shalabi et al. (1979)

ble 3). The adequacy of the model in predicting the asphaltenes and the OGW fractions is clearly shown in this plot.

For the other coals referred to in Table 2, the kinetic results were obtained either using only one solvent to classify the products (Wiser and Hill, 1967; Curran et al, 1967) or using chromatographic method (Mohan and Silla, 1981; Leonard and Silla, 1983) to classify the products. These investigators provide no data on the fractional yields of asphaltenes and OGW fractions obtained during liquefaction of their respective coals. Hence the model predictions for these fractions for their coals cannot be tested. However, it is possible to ascertain the validity of the severity index proposed by the model by examining the liquefaction yields obtained at different temperatures.

Figure 13 contains a plot of Wiser and Hill's (1967) data for the formation of benzene solubles obtained for a Utah high-volatile bituminous coal. The experimental results have been plotted on a reactive coal basis estimated to be 93% from their data. The model curve has been obtained using a first-order fit for the formation of benzene solubles. The fit is reasonable, again showing that the present definition of reaction severity index is adequate.

The product yield obtained from chromatographic separation method for Illinois No. 6 coal (Mohan and Silla, 1981) has been compared with the product yield for Kentucky No. 6 coal (Leonard and Silla, 1983) and found to show a great variation. In Figure 14 both these data have been plotted together using the present definition of severity index (Eq. 3); the differences in the product yields are less apparent. While the multifunctional group shows a poor trend, the hydroxyl and ether yields obtained for the two coals at the same severity are comparable. It should be borne in mind that these two coals had a considerable difference in their elemental composition, and if differences in the

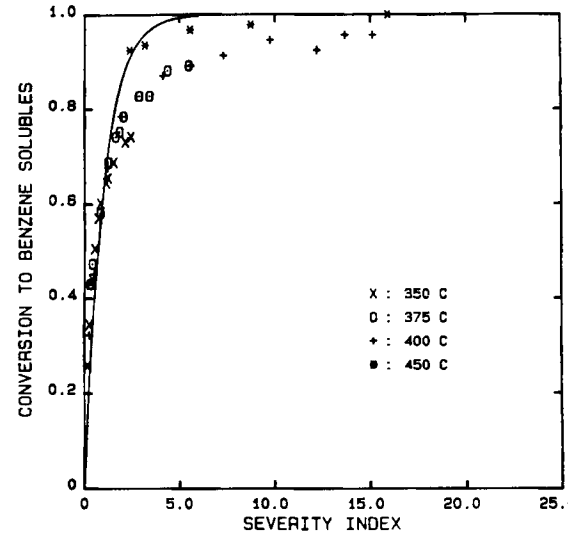

Figure 13. Model fit for conversion.
Utah coal; Hill and Wiser (1967)

functionalities of the two coals existed, these will be most apparent in the multifunctionals fraction.

Temperature effects

Table 4 contains a summary of the reactive portions estimated from the experimental data for all the coals studied as

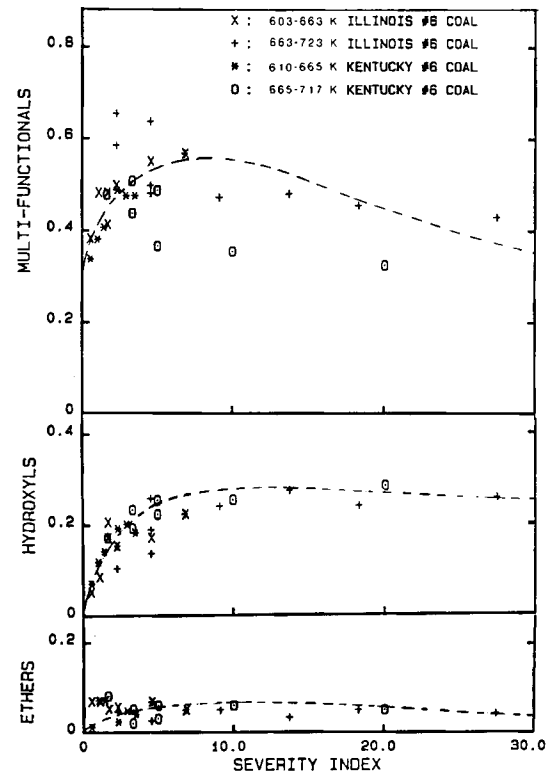

Figure 14. Comparison of product yields at equivalent reaction severity indices.
Lines show trends.
Illinois No. 6 coal (Mohan and Silla, 1981)
Kentucky No. 6 coal (Leonard and Silla, 1983)

Table 4. Reactive Portion and First-Order Rate Constant for Coal Dissolution

Coal	Catalyst	Temp. K	Reactive Frac. wt. % DAF Basis	Rate Constant $s^{-1} \times 10^4$
Morwell	none	588	100	1.09
		608		1.80
		648		4.00
		668		7.56
		688		18.62
	Fe	648	100	4.06
		668		11.25
		688		19.73
	Fe/Sn	648	100	5.08
		668		13.20
		688		25.10
Wandoan	none	653	91	5.65
		673		11.80
		693		35.10
Taroom	none	673	93	17.68
		693		62.03
Kentucky #9 (Shalabi et al., 1979)	none	623	87	2.30
		648		9.00
		673		21.75
Kentucky #6 (Leonard and Silla, 1983)	none	(610–665)	84	9.78
		(665–717)		55.80
Illinois #6 (Mohan and Silla, 1981)	none	(603–663)	88	19.22
		(663–723)		74.82
Pittsburg (Curran et al., 1967)	none	587	90	4.65
		627		9.68
		661		32.40
Utah hVB (Wiser and Hill, 1967)	none	623	93	0.52
		648		1.15
		673		4.07
		723		13.25
Pittsburg #8 (Brooks et al., 1983)	none	723	100	9.70
	Pyrite	723	100	26.68
Liddell (Rottendorf and Wilson, 1980)	none	673	92	1.37
	3% Ni-Mo	673	92	1.42
	5% Ni-Mo	673		1.80
	10% Ni-Mo	673		2.63

well as the first-order rate constants that best fitted the conversion-time data at the respective temperatures. Based on these rate constants, Arrhenius plots for the temperature dependency of all the coals are shown in Figure 15. Where a nonisothermal reaction condition was employed (Mohan and Silla, 1981; Leonard and Silla, 1983), an arithmetic average temperature has been used for the purpose of constructing the plot. All the rate parameters were estimated using an IMSL (1982) routine based on a Levenberg-Marquardt algorithm.

The Arrhenius plot for the rate constants for brown coal yielded an activation energy of 93 kJ/mol for coal dissolution. This value is comparable to the reported value for a Texas lignite (Haley et al., 1981). Figure 15 shows that the Utah, Kentucky No. 9, Wandoan, and Taroom coals exhibit progressively

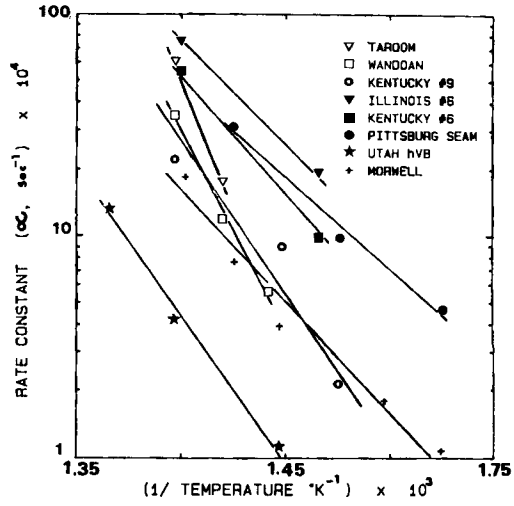

Figure 15. Arrhenius plot of first-order rate constant (α) for coal dissolution.

higher temperature dependency with activation energy increasing from ca. 120 to 200 kJ/mol. The rate parameters for Illinois No. 6 and Kentucky No. 6 coals follow a different temperature dependency with an activation energy of 85 kJ/mol. The similar values for the activation energies within a group of coals indicates that similar types of bonds are broken for these coals, probably reflecting similar basic unit structures.

There appears to be a direct correlation between activation energy and elemental (H/C) ratio for these coals, Figure 16. Since this ratio would give an indication of the degree of condensed ring structures in coal, one could explain the relationship in terms of the strength of bonds broken. The large variation in activation energies for the rate parameters obtained from these coals indicates that comparison of reactivity of different coals should include the temperature effects as well. At low temperatures, brown coals would exhibit rates of formation of THF solu-

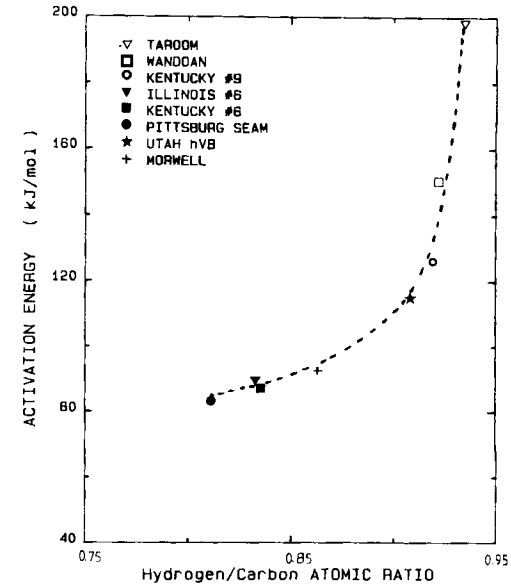

Figure 16. Dependency of activation energy for coal dissolution on atomic (H/C) ratio of coal.

bles comparable to those of black coals, and at high temperatures black coals would display much higher reactivity.

Effect of added catalysts

Brown Coals. Work on brown coal catalysis using iron and iron/tin catalysts shows significant activity when the catalysts are in a highly dispersed form, using ion-exchange methods (Agnew et al., 1984). The results obtained from the continuous reactor (Agnew et al.) using 3:1 tetralin to coal reveal a higher rate of conversion to THF soluble products as well as a higher rate of formation of oils. The fractions of asphaltenes and preasphaltenes formed show similar trends at higher temperature runs. As shown in Figure 17, the product yields obtained at a particular conversion are not dependent upon the presence of catalysts.

The exact role of catalysts in coal liquefaction in an environment where there is an excess amount of a good donor solvent (tetralin) is not clear. The role of catalysts is often associated with aiding hydrocracking reactions (Vernon, 1980) or providing an effective medium for transferring molecular hydrogen from gas phase to the thermally fragmented coal (Watanabe et al., 1984). Marshall et al. (1982) attributed the higher conversions obtained with iron/tin catalysts to an enhancement in the conversion due to contributions from gas phase hydrogen. Since the model proposed is based on the assumption that thermal cracking reactions are involved in the rate-controlling step, one would expect the model to be valid for runs carried out with catalysts in the presence of a good donor solvent. Allowance for the presence of catalysts is made via the first-order rate constant α for the formation of THF soluble product. All other model parameters are kept constant.

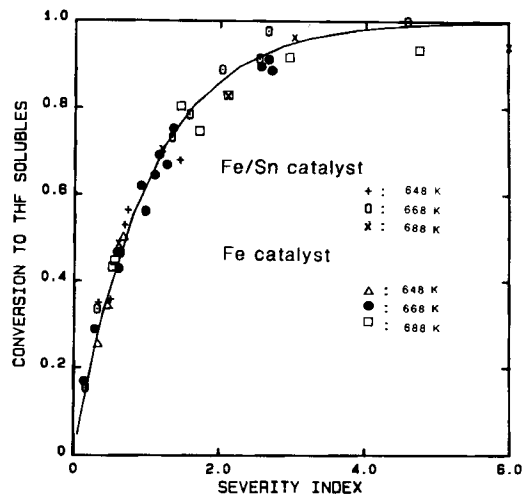

Figure 18. Model fit for conversion.
Mowell coal, Fe and Fe/Sn catalysts.

Figure 18 shows a plot of conversion to THF solubles as a function of reaction severity index both for iron- and iron/tin-catalyzed runs. Included in this plot is the theoretical curve obtained from a first-order rate model for the formation of THF solubles. The rate constant was estimated as before, using an IMSL routine and is summarized in Table 4. The rate constant α obtained for the formation of THF solubles when catalysts were present is higher than the corresponding results for the uncatalyzed liquefaction of brown coal, Table 4. This higher value of rate constant results in a correspondingly higher value for the reaction severity index; see Eq. 3.

Figures 19 and 20 contain plots of preasphaltenes, asphal-

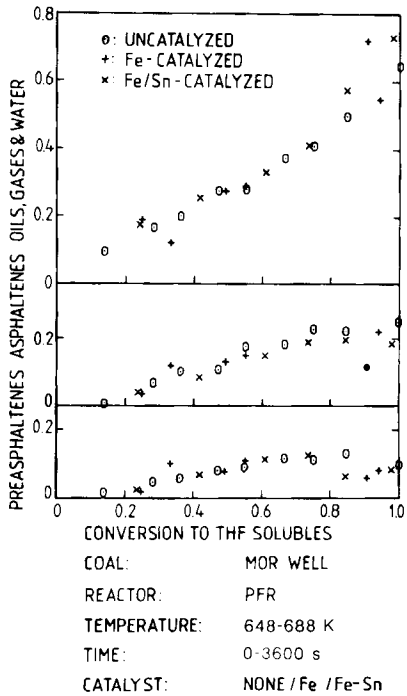

Figure 17. Product yields vs. conversion for Morwell coal.
Effect of catalyst.

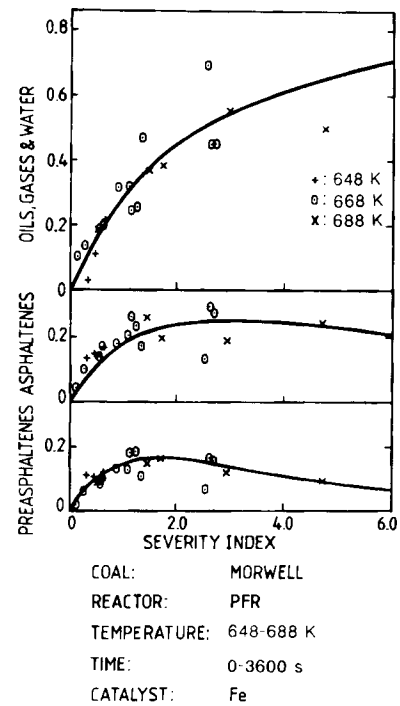

Figure 19. Model fit for product yields.
Morwell coal, Fe-catalyst

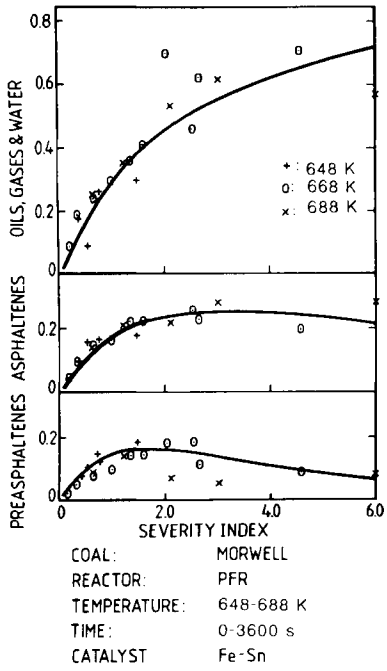

Figure 20. Model fit for product yields.
Morwell coal, Fe/Sn catalyst

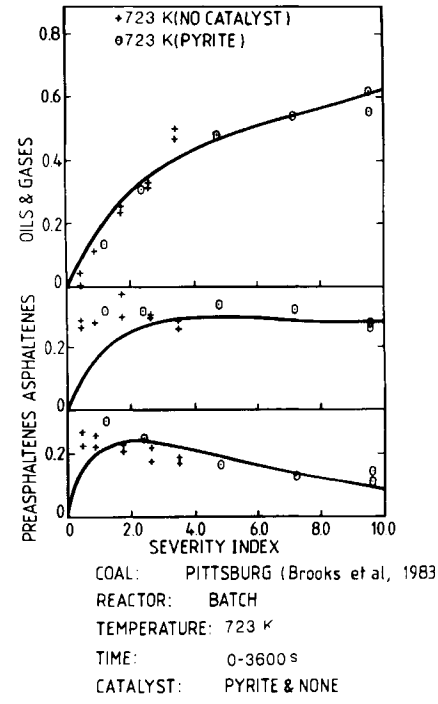

Figure 21. Model fit for product yields.
Pittsburg coal; Brooks et al. (1983).

tenes, and OGW fractions respectively obtained for iron- and iron/tin-catalyzed experiments. The model-predicted profiles (shown as solid lines in these figures) fit the experimental data well. From these plots it would seem that the severity index adequately allows for the effect of catalyst.

Other coals. Brooks et al. (1983) reported conversion and product yield as a function of time at 723 K for a Pittsburg coal in a light recycle solvent studying the effect of added pyrite catalysts. The rate constant has been obtained for the case of uncatalyzed liquefaction and pyrite-catalyzed liquefaction and is shown in Table 4. Using the corresponding reaction severity index for these two cases, Figure 21 has been constructed. With the data plotted in this form, the differences between catalyzed and uncatalyzed runs are less, which again shows that the pyrite catalyst promotes all the reactions equally, even for a light recycle solvent. The plot also contains the model-predicted profiles using an assumed molecular weight of 1,328 ($u = 100, v = 8$) for this coal.

Rottendorf and Wilson (1980) studied the liquefaction behavior of Liddell coal (Australia) and the effect of a commercial Ni-Mo hydrodesulfurization catalyst on the formation of liquid products and the yield of tetralin solubles. Based on the assumption of the solid residue to be essentially unreacted coal, first-order rate contant was obtained for the different catalyst loading and this was used in constructing Figure 22 for the formation of tetralin soluble products vs. reaction severity index. Once again our definition of severity index is shown to be adequate in combining the effects of temperature and time for different catalyst loadings. Since Rottendorf and Wilson did not use a three-solvent method to characterize their products, comparison with the model was not possible.

Temperature Effects. The presence of catalyst seems to alter the rate of formation of THF soluble products by changing the selectivity to any one group of lumped products. This would imply that all reactions are speeded up to the same extent. The Arrhenius plot of the rate constants for catalyzed liquefaction are shown in Figure 23. For the brown coal studied the rate parameters for both iron-catalyzed and iron/tin-catalyzed runs follow a similar temperature dependency (i.e., the same activation energy) as uncatalyzed liquefaction. Thus the only alteration seems to be an effective increase of the reaction temperature. This finding, at least in the presence of a good donor solvent, has important implications, since if the selectivity is not altered by catalyst addition there is little advantage to be gained

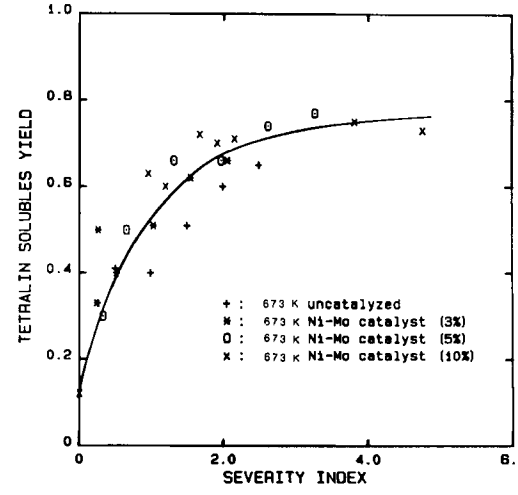

Figure 22. Effect of catalyst loading on product yield for Liddell coal.
Rottendorf and Wilson (1980)

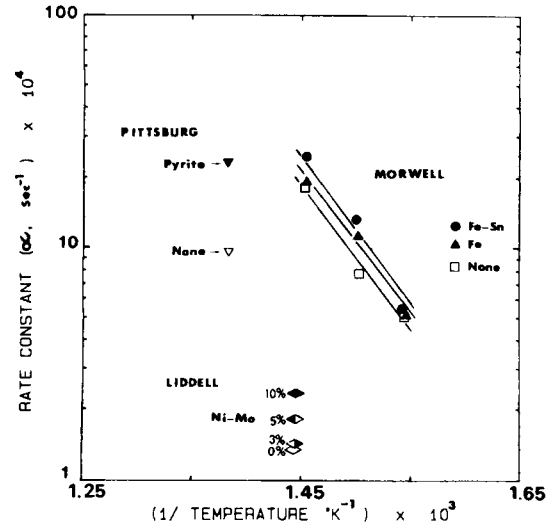

Figure 23. Arrhenius plots of first-order rate constant (α) for coal dissolution.
Effect of catalyst.

in terms of an increased rate of conversion. This conclusion is in broad agreement with that of Kang (1983).

Analytical expression for product yields for all coals

The general shape of the product yields predicted for all the coals examined (Figures 7, 10, 11, 12, 19, 20, and 21) indicates a fundamental similarity of these profiles. Since the characteristic molecular weight of coal is the only parameter that varied between coals, the theoretical profiles can be fitted by the following analytical equations:

$$\text{Coal} = \exp(-a \cdot \theta) \tag{5}$$

$$\text{Preasphaltenes} = \frac{K_1}{(a-b)}\exp(-b \cdot \theta) + \frac{K_1}{(b-a)}\exp(-a \cdot \theta) \tag{6}$$

$$\text{Asphaltenes} = \frac{K_2}{(a-K_6)}\exp(-K_6 \cdot \theta) + \frac{K_2}{(K_6-a)}\exp(-a \cdot \theta) + \frac{K_4 \cdot K_1}{(b-K_6)(a-K_6)}\exp(-K_6 \cdot \theta) + \frac{K_4 \cdot K_1}{(a-b)(K_6-b)}\exp(-b \cdot \theta) + \frac{K_4 \cdot K_1}{(b-a)(K_6-a)}\exp(-a \cdot \theta) \tag{7}$$

$$\text{OGW} = 1 - (\text{Coal} + \text{Preasphaltenes} + \text{Asphaltenes}) \tag{8}$$

where,

$$a = K_1 + K_2 + K_3 \quad \text{and} \quad b = K_4 + K_5 \tag{9}$$

the constants (K_i's) are related to the molecular weight (M_w) of coal:

$$\begin{aligned} K_1 &= 1.19\exp(-1{,}475/M_w) \\ K_2 &= 0.1254\exp(1{,}053/M_w) \\ K_3 &= 0.1317\exp(1{,}125/M_w) \\ K_4 &= 0.0552\exp(375/M_w) \\ K_5 &= 0.0104\exp(3{,}203/M_w) \\ K_6 &= 0.0245\exp(1{,}282/M_w) \end{aligned} \tag{10}$$

Equations 5 to 9 allow calculation of the yield profiles using the parameter values of Eq. 10 without the need to use the continuum model, with deviations not exceeding 3%. The only unknown in Eq. 10 is the characteristic molecular weight for coal. At this stage there does not seem to be a simple method of determining M_w.

Acknowledgment

The authors wish to gratefully acknowledge funds provided under the National Energy Research, Development, and Demonstration Program, which is administered by the Commonwealth Department of National Development and Energy. G. N. Prasad was supported by a Commonwealth postgraduate research award. R. T. White and P. Thewlis were responsible for obtaining the kinetic data from the continuous reactor unit for Morwell coal.

Notation

(Other terms are defined in Part I Notation.)

$K_1, K_1, K_3, K_4, K_5, K_6$ = parameters, Eq. 10, dimensionless
$\overline{M_c}$ = molecular weight between crosslinks in coal (after Lucht and Peppas, 1984)
M_w = characteristic molecular weight of coal
n_i = number of repeated runs at the same conditions
OGW = oils, gases, and water.
SI = severity index.
T = reaction temperature
THF = tetrahydrofuran
α = rate constant for formation of THF solubles, s^{-1} (= rate kernel for coal, Part I)
θ = reaction severity index (= $\alpha \cdot t$), dimensionless (= dimensionless time, Part I)

Literature cited

Agnew, J. B., W. R. Jackson, F. P. Larkins, D. Rash, D. E. Rogers, P. Thewlis, and R. White, "Hydroliquefaction of Victorian Brown Coal in a Continuous Reactor. 1: Effects of Residence Time Temperature and Catalysts on Conversion," *Fuel*, **63**, 147 (1984).

Aris, R., and G. R. Gavalas, "On the Theory of Reactions in Continuous Mixtures," *Phil. Trans. Royal Soc. London*, **260**, 351 (1966).

Brooks, D. G., J. A. Guin, C. W. Curtis, and T. Placek, "Pyrite Catalysis of Coal Liquefaction, Hydrogenation and Intermolecular Transfer Reactions," *Ind. Eng. Chem. Process Des. Dev.*, **22**, 343 (1983).

Cassidy, P. J., P. A. Hertan, W. R. Jackson, and F. P. Larkins, "Hydrogenation of Brown Coal. 3: Roles of Hydrogen and Hydrogen-Donor Solvents in Systems Catalyzed by Iron and Tin Compounds," *Fuel*, **61**, 939 (1982).

Cochran, S. J., M. Hatswell, W. R. Jackson, and F. P. Larkins, "Evidence for Direct Interaction of Hydrogen with Brown Coal in Tin-Catalyzed Reactions," *Fuel*, **61**, 831 (1982).

Cronauer, D. C., Y. T. Shah, and R. G. Ruberto, "Kinetics of Thermal Liquefaction of Belle Ayr Subbituminous Coal," *Ind. Eng. Chem. Process Des. Dev.*, **17**, 281 (1978).

Curran, G. P., R. T. Struck, and E. Gorin, "Mechanism of Hydrogen-Transfer Process to Coal and Coal Extract," *Ind. Eng. Chem. Process Des. Dev.*, **6**, 166 (1967).

Furlong, M. W., R. M. Baldwin, and R. L. Bain, "Reactivity of Coal Towards Hydrogenation Ranking by Kinetic Measurement," *Fuel*, **61**, 116 (1982).

Given, P. H., R. Schleppy, and A. Sood, "Dependence of Coal Liquefaction Behavior on Coal Characteristics. 5: Data from a Continuous-Flow Reactor," *Fuel*, **59**, 747 (1980).

Gollakota, S. V., and J. A. Guin, "Comparitive Study of Gas-Liquid Mass Transfer Coefficients in Stirred Autoclaves, Tubing Bomb Microreactors and Bubble-Columns," *Ind. Eng. Chem. Process Des. Dev.*, **23**, 52 (1984).

Guin, J. A., A. R. Tarrer, J. W. Prather, D. R. Johnston, and J. M. Lee, "Effects of Coal Minerals on the Hydrogenation, Desulfurization and Solvent Extraction of Coal," *Ind. Eng. Chem. Process Des. Dev.*, **17**, 118 (1978).

Haley, S. K., and J. A. Bullin, "Empirical Models for the Rate of Lignite Liquefaction," *Fuel Process. Tech.*, **4**, 191 (1981).

Han, K. W., V. B. Dixit, and C. Y. Wen, "Analysis and Scale-up Consideration of Bituminous Coal Liquefaction Rate Processes," *Ind. Eng. Chem. Process Des. Dev.*, **17**, 16 (1978).

Han, K. W., C. Y. Wen, "Initial Stage (Short Residence Time) Coal Dissolution," *Fuel*, **58**, 779 (1979).

Holman, J. P., and W. J. Gajda, *Experimental Methods for Engineers*, 3rd ed., McGraw-Hill, New York (1978).

IMSL subroutine, *ZXSSQ*, 9th ed., IMSL Library, Houston (June, 1982).

Jackson, W. R., F. P. Larkins, P. Thewlis, and I. Watkins, "Rapid Extraction of Products from Coal Hydrogenation Reactions Using an Ultrasonic Bath," *Fuel*, **62**, 606 (1983).

Kang, K. C., "Catalytic Conversion of Coal: A Myth or a Truth?," *Proc. 1983 Int. Conf. Coal Sci.*, IEA, Pittsburgh, 75 (1983).

Leonard, E., and H. Silla, "Kinetics of Donor-Solvent Liquefaction of Kentucky No. 6 Coal," *Ind. Eng. Chem. Process Des. Dev.*, **22**, 445 (1983).

Lucht, L. M., and N. A. Peppas, "Crosslinked Structures in Coals: Models and Preliminary Experimental Data," *New approaches in coal chemistry*, B. D. Blaustein B. L. Bockrath, and S. Friedman, eds., *ACS Symp. Ser.*, **169**, Washington, DC 43 (1981).

Lucht, L. M., and N. A. Peppas, "The Molecular Weight Between Crosslinks of Selected American Coals," *ACS Div. Fuel Chem. Prepr.*, **29** (1), 199 (1984).

Marshall, M., W. R. Jackson, F. P. Larkins, M. R. Hatswell, and D. Rash, "A Synergistic Catalytic Effect in the Hydrogenation of Victorian Brown Coals," *Fuel*, **61**, 121 (1982).

Mohan, G., and H. Silla, "Kinetics of Donor-Solvent Liquefaction of Bituminous Coals in Nonisothermal Experiments," *Ind. Eng. Chem. Process Des. Dev.*, **20**, 349 (1981).

Moritomi, H., M. Naruse, H. Nagaishi, Y. Sanada, and T. Chiba, "On the Mechanism and Kinetics of Initial-Stage Coal Liquefaction," *Proc. 1983 Int. Conf. Coal Science*, IEA, Pittsburgh, 134 (1983).

Neavel, R. C., "Liquefaction of Coal in Hydrogen-Donor and Nondonor Vehicles," *Fuel*, **55**, 237 (1976).

Petrakis, L. W., D. W. Grandy, and G. L. Jones, "Free Radicals in Coal and Coal Conversion. 8: Experimental Determination of Conversion in Hydroliquefaction," *Fuel*, **62**, 665 (1983).

Phillip, C. V., and R. G. Anthony, "Chemistry of Texas Lignite Liquefaction in a Hydrogen-Donor Solvent System," *Fuel*, **61**, 351 (1982).

Rottendorf, H., and M. A. Wilson, "Effect of *in-situ* Mineral Matters and a Ni-Mo Catalyst on the Hydrogenation of Liddell Coal," *Fuel*, **59**, 175 (1980).

Sangnimnuan, A., G. N. Prasad, and J. B. Agnew, "Gas Holdup and Backmixing in a Bubble-Column Reactor under Coal Hydroliquefaction Conditions," *Chem. Eng. Commun.*, **25**, 193 (1984).

Shalabi, M. A., R. M. Baldwin, R. L. Bain, J. H. Gray, and J. O. Golden, "Noncatalytic Coal Liquefaction in a Donor Solvent. Rate of Formation of Oil, Asphaltene, and Preasphaltene," *Ind. Eng. Chem. Process Des. Dev.*, **18**, 474 (1979).

Szladow, A. J., and P. H. Given, "Models and Activation Energies for Coal Liquefaction Reactions," *Ind. Eng. Chem. Process Des. Dev.*, **20**, 27 (1981).

———, "Analysis of Coal Dissolution Reaction Engineering," *Chem. Eng. Commun.*, **19**, 115 (1983).

Thewlis, P., R. White, J. B. Agnew, W. R. Jackson, and D. Rash, "Coal Hydroliquefaction Reaction Kinetics," *Abst. and papers, 8th Australian Workshop Coal Liquefaction*, Melbourne, 77 (1983).

Tsai, M. C., and S. W. Weller, "Catalysis of Hydrogen Transfer in a Tetralin-Coal System," *Fuel Process. Tech.*, **2**, 313 (1979).

Vernon, L. W., "Free Radical Chemistry of Coal Liquefaction: Role of Molecular Hydrogen," *Fuel*, **59**, 102 (1980).

Watanabe, Y., O. Yamada, K. Fujita, Y. Takegami, and T. Suzuki, "Coal Liquefaction Using Iron Complexes as Catalysts," *Fuel*, **63**, 752 (1984).

White, R. T., P. Thewlis, and J. B. Agnew, "Continuous Hydroliquefaction of Victorian Brown Coal—Catalytic Studies," *Abst. and papers, 7th Australian Workshop Coal Liquefaction*, North Ryde, Sydney, 114 (1982).

Wiser, W. H., and G. R. Hill, "A Kinetic Study of the Thermal Dissolution of High-Volatile Bituminous Coal," *Proc. Symp. Sci. Tech. Coal*, Ottawa, 162 (1967).

Zieminski, G. H., "Rate Limitations in Coal-Organic Solvent Interactions," Ph.D. Diss., Univ. California, Berkeley (1982).

Manuscript received in two parts, Apr. 10, and Apr. 23, 1985, and revision received Dec. 11, 1985.